Fractal structure of the complete devil's staircase in dissipative systems described by a driven damped-pendulum equation with a distorted potential

P. Alstrøm and M. T. Levinsen
Physics Laboratory I, H.C. Ørsted Institute, Universitetsparken 5, DK-2100 Copenhagen Ø. Denmark
(Received 17 December 1984)

The universality of the fractal structure of the complete devil's staircase found for a driven damped-pendulum equation is tested against distortion of the potential. The fractal dimension is found to be independent of the exact form of the potential. The different decay exponents for the step sequences $1/Q$, the Fibonacci, and P/Q averaged over P are also found to be independent of the potential. The detailed behavior of the I-V curves can, however, be appreciably affected. Nonetheless, the step widths found along the critical line still form a self-similar staircase very nearly symmetric around the $1/2$ step. The results mean that the universality may be studied in systems such as Josephson tunnel junctions with external resistive shunts, microbridges, or *SNS* junctions with external capacitive shunts, Josephson point contacts, or sliding charge-density-wave systems.

I. INTRODUCTION

In some recent papers Bak *et al.*[1,2] have discussed the two-dimensional return map for the differential equation for a damped pendulum driven with a periodic torque with a constant offset. They showed, that in a parameter regime including the transition to chaos the return map collapses to a one-dimensional Poincaré map, e.g., a circle map. A specific prediction was that the complete devil's staircase encountered along the transition to chaos should have a fractal dimension of $D=0.87$. Furthermore, the return map will have a zero-slope inflection point of order three along the critical line. For the sinusoidal nonlinear potential this behavior has been verified both locally[3] and globally[4,5] in analog computations on the pendulum equation. There are, however, still some outstanding questions of interest not only from a theoretical point of view but also with respect to possible experiments. Namely, what if any are the changes in the return map and in the critical line resulting from a distortion of the potential from the sinusoidal form? Obviously the answers are very important in the analysis of experiments, both for an experimental verification of the universal properties and for using these properties as a tool for a better understanding of the dynamics of the specific system under investigation.

What is meant by universal properties is that the system belongs to a universality class represented by a discrete circle map with a specific choice of order of the inflection point.[6]

Experimentally the interest has centered on two different systems. It has long been known that subharmonic steps show up in the I-V characteristics for the resistively-shunted Josephson-junction model (RSJ model) when a shunt capacitance was included.[7,8] Such substeps have also often been observed experimentally.[9] It is, however, rather difficult to make Josephson junctions with such parameters, that a complete devil's staircase may be investigated in sufficient detail. A completely different possibility is presented by the sliding charge-density-waves in rf fields as found in certain linear chain compounds, e.g., $NbSe_3$. The I-V curves without the presence of an ac drive has been shown to fit the Josephson equation with a sinusoidal "current-phase" relation.[10] Based on the frequency-dependent conductivity below threshold the inertial term should always be negligible and the system therefore overdamped. However, judging from the behavior at finite voltages there seem to be two distinct temperature regimes with the system overdamped above ~ 40 K and underdamped below.[11] In the former regime subharmonic locked current steps, which apparently make up a complete devil's staircase, were recently observed and a fractal dimension of $D=0.91\pm0.03$ was reported.[12] In the latter case the Feigenbaum bifurcation sequence to chaos was observed on the harmonic steps.[11] Both results indicate that the low value of the inertial term has to be modified. Still analog calculations show that the I-V curves lie above the critical line for the transition to chaos for the former case. It is therefore highly surprising that a complete devil's staircase should be encountered. However, one should be careful not to infer too much about the current-phase relationship from the dc I-V curves obtained without an ac drive. A nonsinusoidal relation may in fact give exactly the same I-V curve as a sinusoidal current-phase relation, as we shall show in the following. Such a nonsinusoidal relationship is known to be able to generate substeps even in the absence of an inertial term.[13] Hence one might speculate that an enhancement of the substeps could occur with both causes working together. We have therefore undertaken an analog computer investigation of the driven pendulum equation with a nonsinusoidal potential.

From inspection of the return map one might naively relate the behavior of the return map to the properties of the current-phase relation. This naive notion is, however, false. We have investigated a periodic current-phase relation with a fifth-order inflection point in order to prove this. In this case, as well as in the case of a skewed current-phase relation, we find a fractal dimension and

decay constants within the experimental uncertainty to agree with the results on the discrete circle map with a third-order inflection point.

Finally we have considered the question of self-similarity. Since the connection between the dc drive (in units of which the widths of substeps are measured) and the parameter

$$\Omega=\frac{1}{2\pi}\int_0^{2\pi}\phi((n+1)\tau)d\phi(n\tau)-\pi$$

of the return map is far from obvious, it is actually somewhat surprising that the fractal dimension, when measured globally between the 0/1 and 1/1 steps, comes out right. Even more surprising is that the fractal dimension $\overline{D}$ found by considering the P average over the P/Q substeps for all the cases we have considered is identical to $D=0.87$ within the experimental uncertainty. A plot of the widths of the substeps between the 0/1 and 1/1 steps reveals that the step structure is truly self-similar. Indeed, it is very nearly symmetric around the 1/2 step even though the dc drive may vary both up and down along the critical curve.

II. THE CURRENT-PHASE RELATION

Both the Josephson junction and the sliding charge-density-wave (CDW) can at least approximately be described by the equation for a damped pendulum driven by a constant plus a periodic torque. We shall write the equation in the normalized form commonly used for the Josephson junction. The equations for the phase difference ϕ and the voltage $V(t)$ are then

$$\ddot{\phi}+G\dot{\phi}+I(\phi)=I+A\sin(\omega t)\ ,$$

and (1)

$$V(t)=G\dot{\phi}\ ,$$

where $I(\phi)$ is a periodic function. In the case of the CDW currents and voltages are interchanged.

In Eq. (1) the current-phase relation $I(\phi)$ is normally taken to be sinusoidal. In most Josephson tunnel junctions this is very well satisfied. However, when the tunneling barrier is either very thin or very low, higher-order tunneling terms become important. Terms of the form $\sin n\phi$, where n is a positive integer, are then introduced. These terms show up in the I-V curves through subharmonic steps and subgap structures.[14,15] In Josephson microbridges similar terms may be occasioned by the kinetic inductance of the Cooper pairs or simply by the junction being physically too large compared to the coherence length.[16] Subharmonic steps have been observed in great numbers in microbridges.[17] It is therefore of interest to investigate the changes resulting from a nonsinusoidal current-phase relation already from the viewpoint of Josephson junctions. Here, we will not speculate on the form of $I(\phi)$ for the CDW, which is still an open issue.[18] Let us simply point out that nonsinusoidal $I(\phi)$ relations can be constructed in such a way that at least for high-G values and $A=0$ the I-V curve is left unchanged. The current-phase relation, which we will now discuss, has been chosen with this in mind.

The I-V curve for $G\gg1$ and no ac current applied can be calculated exactly by remembering that the period in time is given by [for $I(\phi)=\sin\phi$]

$$T=\int_{-\pi}^{\pi}\frac{Gd\phi}{I-\sin\phi}\ , \tag{2}$$

the dc voltage is then $V\equiv 2\pi G/T=(I^2-1)^{1/2}$. Let us now substitute $I_B(\phi)=\sin(\phi+B\sin\phi)$ for $I(\phi)=\sin\phi$. For $-1<B<1$ we obtain a skewed current-phase relation as shown in Fig. 1 ($B=0.25$) with no new zero crossings. The period in time is now given by

$$\begin{aligned}T&=\int_{-\pi}^{\pi}\frac{Gd\phi}{I-\sin(\phi+B\sin\phi)}\\&=\int_{-\pi}^{\pi}\frac{Gd\phi(1+B\cos\phi)}{I-\sin(\phi+B\sin\phi)}\ ,\end{aligned} \tag{3}$$

where the last equality is true because of symmetry. The change of variables $\phi+B\sin\phi\rightarrow\phi$ brings us back to Eq. (2) and T, and therefore the I-V curve is unchanged.

Let us now consider the two limiting cases of simple $I(\phi)$ relations, namely the triangular and the square. In both cases the I-V curves can easily be calculated by use of Eq. (2). For the former we have

$$V=2\ln[(I+1)/(I-1)]$$

and for the latter $V=(I^2-1)/I$, with $V=(I^2-1)^{1/2}$ for the sinusoidal case lying in between. For the triangular $I(\phi)$ relation a similar symmetry argument as used for $I_B(\phi)$ again gives that the I-V curve is indifferent to the symmetry of the $I(\phi)$ relation. We should mention here that a triangular $I(\phi)$ relation has some interest since this could explain the constant plasma frequency in the CDW.

We will now turn to the case of a combined dc and ac drive. Why do we expect subharmonic steps even for $G\gg1$ in the case of the skewed $I(\phi)$ relation? Using a Bessel function expansion we can write

$$I_B(\phi)=\sum_{n=-\infty}^{\infty}J_n(B)\sin(\phi+n\phi)\ .$$

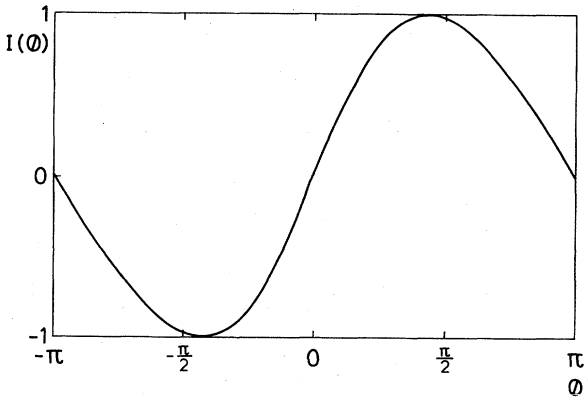

FIG. 1. The skewed current-phase relation, $I_B(\phi)=\sin(\phi+0.25\sin\phi)$.

The subharmonic steps are now created by the beating of these higher-order terms with the applied ac drive, thus destroying the delicate balance that gives the substeps amplitude zero in the sinusoidal case. The changes brought about by $I(\phi)$ will be the topic of the next two sections. In Sec. V we will discuss the following $I(\phi)$ relation:

$$I_5(\phi)=\tfrac{6}{7}[\sin\phi+\tfrac{1}{6}\sin^3(\phi)]\ . \tag{4}$$

This has the property of a fifth-order inflection point at the origin. The reason to discuss this relation will become clear later on.

III. THE CRITICAL LINE

Equation (1) was investigated by the use of an analog computer (EAI 680). The $\sin(\omega t)$ and the $I(\phi)$ terms were both produced on the computer[5] by amplitude stabilized circuits which permitted operation of the computer in the continuous mode and allowed for an easy time-scale change. A sweep oscillator was used for tracing out I-V curves with G, A, and ω as parameters. For fixed values of I, G, A and ω, return maps could easily be constructed by simultaneously plotting $I(\phi)$ and $\sin(\omega t)$ as functions of $\phi(t)$, or alternatively by plotting $\phi(t)$ and $\sin\omega t$ as functions of t and $I(\phi)$ as a function of $\phi(t)$. An example of this second approach is shown in Fig. 2. The parameters $A=1$ and $\omega=1.76$ are used almost exclusively in the remainder of this paper, when ac drives are present. The dc current and the damping factor are chosen to illustrate the behavior of $\phi(t)$ at the critical line. For the specific values used here the point on the I-V curve is just below the 1/7 substep. By the critical line in (I,G) space we understand the line consisting of the points in (I,V) space below but not above which the I-V curve shows hysteresis and chaotic behavior. A more precise definition is given in Ref. 5. A return map can now be constructed by plotting for successive periods of the ac drive at times $t_n=2\pi n/\omega+t_0$ the corresponding values of $\phi(t)$, each as function of the preceding value, i.e., (ϕ_{n+1},ϕ_n). Figures 3(a) and 3(b) illustrate that the critical line can be moved

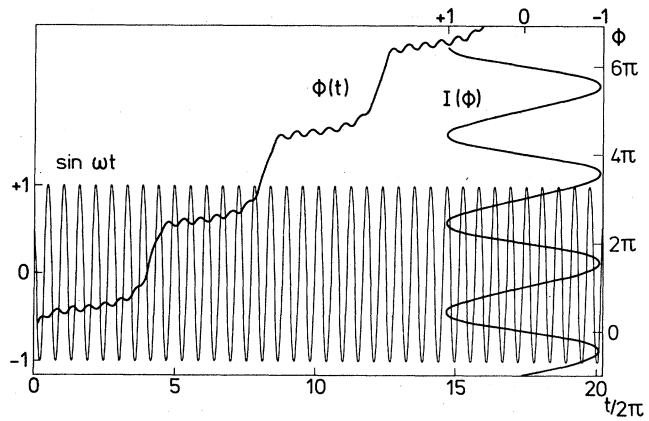

FIG. 2. Composite picture where $\sin(\omega t)$ (horizontal) and $I(\phi)$ (vertical) establish a grid on which the return map $\phi_{n+1}=\phi(2\pi(n+1)/\omega+t_0)$ as a function of $\phi_n=\phi(2\pi n/\omega+t_0)$ can be constructed. $G=1.64$, $I=1.06$, $A=1$, and $\omega=1.76$.

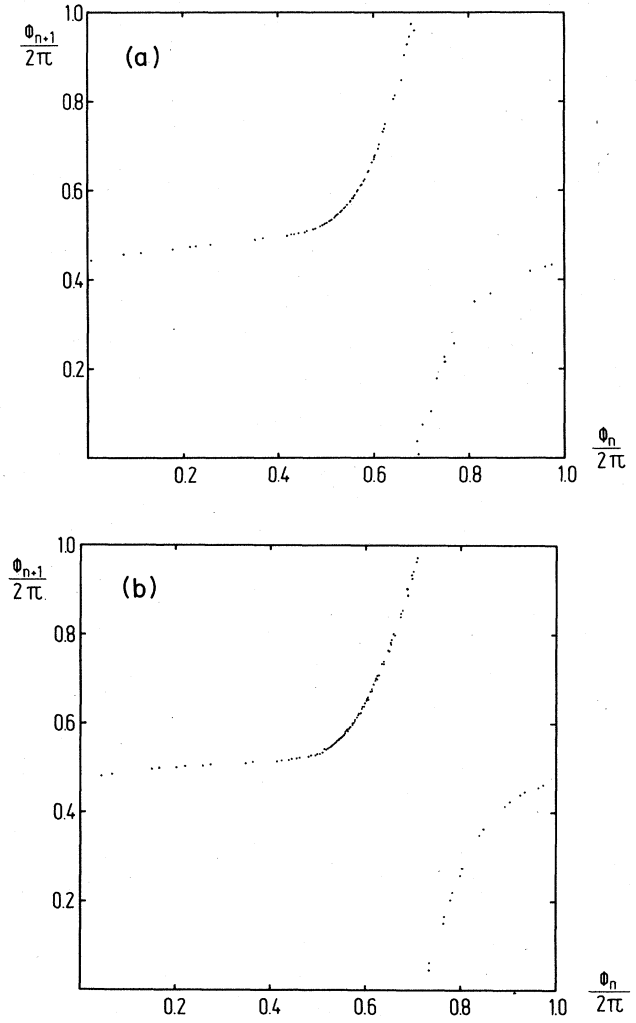

FIG. 3. Return map at a rotation number just below $W=1/7$ in the limit $A=0$ for (a) $I(\phi)=\sin\phi$. (b) $I_B(\phi)=\sin(\phi+0.25\sin\phi)$. Note that the slope at the inflection point on the plateau has been lowered.

towards higher values of G and I by a nonsinusoidal $I(\phi)$. Figure 3(a) shows a return map obtained for $I(\phi)=\sin\phi$, while Fig. 3(b) shows a return map for $I(\phi)=\sin(\phi+B\sin\phi)$ with $B=0.25$. The return maps are obtained in the limit $A\to 0$. Except for this all parameters are the same as in Fig. 2. It is seen that the slope at the inflection point on the plateau has been lowered noticeably. Thus, even though within the experimental uncertainty the I-V curves are identical, the return map is clearly changed in such a way as to expect that the critical line has moved closer.

In order to show the overall change in the I-V curves occasioned by using a skewed $I(\phi)$ relation, we have traced out sets of I-V curves for $A=1$, $\omega=1.76$, and the values $B=0$ [Fig. 4(a)], and $B=0.25$ [Fig. 4(b)] with G as a parameter. As predicted the substeps are much more

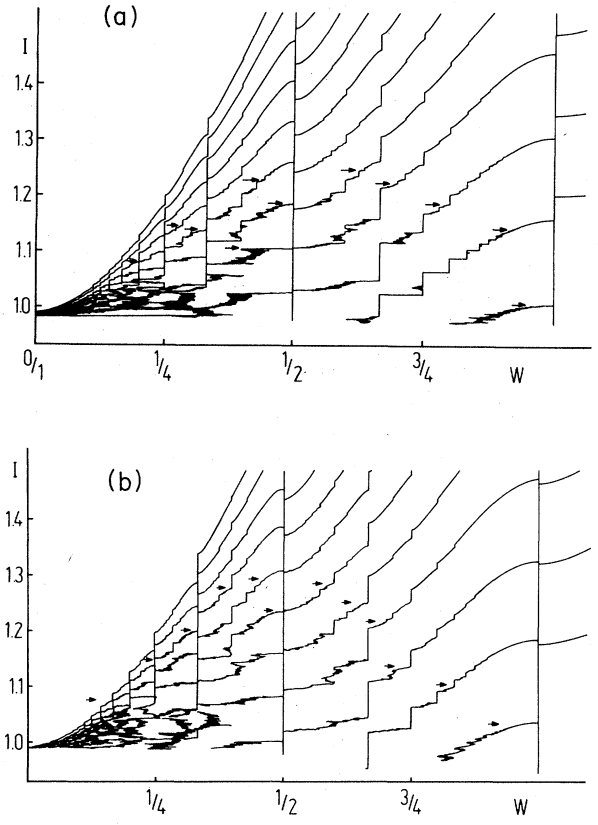

FIG. 4. I-V curves obtained for $A=1$ and $\omega=1.76$. The damping factor G is lowered successively by $\Delta G=0.08$ starting with $G=1.6$. Critical points are indicated by arrows. (a) $I(\phi)=\sin\phi$. (b) $I_B(\phi)=\sin(\phi+0.25\sin\phi)$. Note that the arrows indicating the critical line has moved up in current.

prominent with $B=0.25$ and the critical line (marked with arrows where it cuts across the I-V curves) has moved up in current. The occurrence of hysteresis and chaos on the I-V curve below the critical point can be understood as a result of overlaps between a multitude of subharmonic steps of infinitely-low binding energy. Since for $G>1$ the I-V curves without the ac drive are identical within the experimental uncertainty for $-1<B<1$, and the substeps with the ac drive turned on are enhanced by skewing over the $I(\phi)$ relation (B positive), it is easy to understand why the hysteresis sets in for higher G values with $B>0$.

Above the critical line the staircase is not complete. When biased between steps the two basic frequencies, the Josephson frequency and the external drive frequency, are incommensurable. Thus $\phi(t)$ never repeats itself (as seen from the return map). Nevertheless, in the frequency domain we have a discrete spectrum consisting of the frequencies $n\langle\dot{\phi}\rangle+m\omega$, n and m integers. Below the critical line the staircase is overcomplete. The phase wanders apparently aimlessly around. This is illustrated in Fig. 5 where $\phi(t)$ is shown for a situation well within the chaotic regime. In this case a strange attractor is present and small perturbations can lead to wildly different solutions

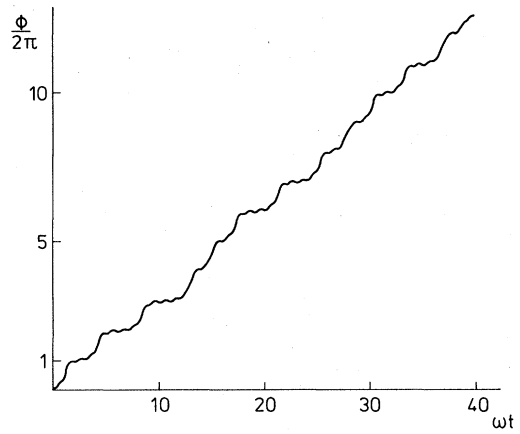

FIG. 5. Development of the phase with time deep inside the chaotical regime. Note the irregular behavior.

for $\phi(t)$. External noise pulses can trigger these wanderings between the very loosely bound substeps, and thus result in a seemingly high noise output even at very low frequencies.

The critical lines have been studied in more detail by tracing out enlarged portions around the critical points with G as a parameter. In Fig. 6 is shown the critical lines obtained for the situation in Figs. 4(a) and 4(b). The critical lines are followed for $0/1<W<1/1$, where W is the rotation number $W=\langle\dot{\phi}\rangle/\omega$. The critical line is ob-

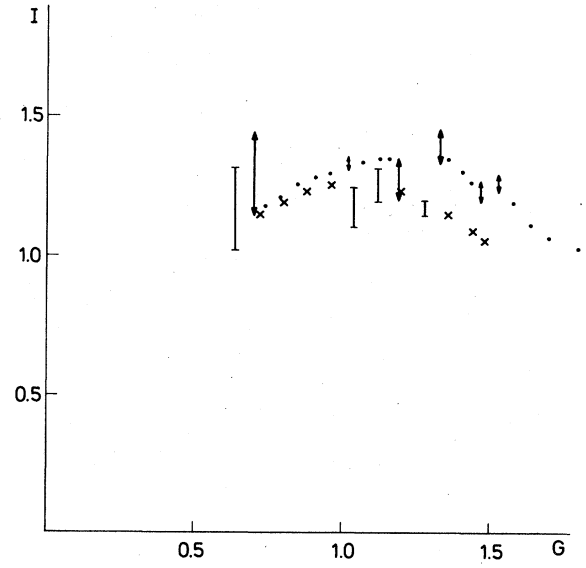

FIG. 6. Critical points in the (I,G) space. Intervals are given where hysteresis is found below but not above a step. $A=1$ and $\omega=1.76$. ($\times$, I) belongs to $I(\phi)=\sin\phi$, (●,↕) belongs to $I_B(\phi)=\sin(\phi+0.25\sin\phi)$. The major steps are $W=1/1$ and $1/2$.

served to lie appreciably higher for $B=0.25$ than for $B=0$ in the regime $G>1$. Here the creation of subharmonic steps is dominated by the nonsinusoidal $I(\phi)$ relation. For low G values the critical lines run together. This, however, does not mean that the I-V curves become identical as can been seen from Figs. 4(a) and 4(b).

From the measured value of the plasma frequency one finds $G\sim 10$ and $\omega\sim 0.01$ for the CDW measurements by Brown *et al.*[12] in which a complete staircase apparently was observed. However, our analog calculations show that for these parameters the substeps do not appear. Even though there is a distinct change from $G\sim 1.5$ to $G=1.8$ in the highest value of G where a critical point can be observed in the data of Figs. 4(a) and 4(b), a skewed $I(\phi)$ relation cannot alone explain the results of Brown *et al.*[12] In light of the measurements of Hall *et al.*,[11] an obvious conclusion is that the damping for finite currents is different from the damping below threshold. There is the additional complication that the I-V curve, in the region where the substeps are observed, has the wrong curvature as compare to that of the resistively shunted junction (RSJ) model. In fact $I\sim(V-V_T)^\gamma$ with $1<\gamma<2$ (Ref. 18) for the CDW system, while $I\sim(V-V_T)^{1/2}$ using the RSJ model ($V-V_T\ll V_T$). We feel that the different curvature and the existence of the substeps are probably related. We have therefore refrained from a more detailed comparison until a firmer theoretical basis is obtained for the dynamics of the CDW in the relevant region. At the moment there exist several competing theories,[18] none of which, however, are easily cast into a differential equation that we can solve on the analog computer.

We have also checked the idea that the transition point is determined by the return map having slope zero at the inflection point. A return map corresponding to the critical point, for which $\phi(t)$ is displayed in Fig. 2, is shown in Fig. 7. Indeed we find that the slope at the inflection point is zero within the experimental uncertainty as expected.

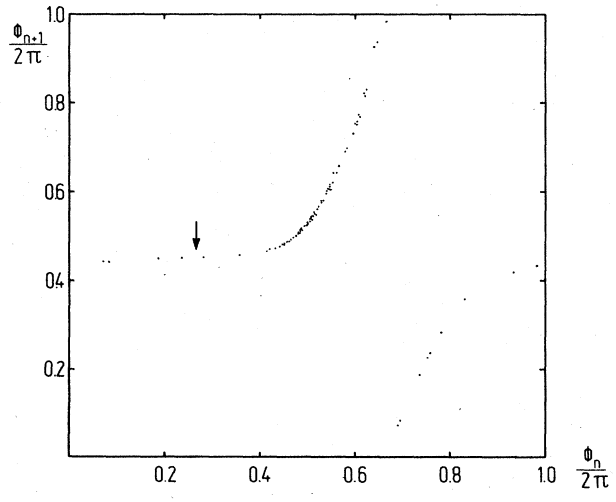

FIG. 7. Return map at the critical point just below the 1/7 substep for $I_B(\phi)=\sin(\phi+0.25\sin\phi)$. Parameters $I=1.06$, $G=1.64$, $A=1$, and $\omega=1.76$. Note the inflection point with slope zero as marked by the arrow.

A still not completely settled question is whether the critical line itself has a fractal structure. Calculations on a standard discrete dissipative map indicate that this is not the case.[2] From more detailed measurements than those displayed in Fig. 6 we arrive at the same conclusion.

IV. THE FRACTAL STRUCTURE

On the enlarged portions of the I-V curves used to obtain the critical line we can also measure the size of the substeps following the critical line. As in the case of $B=0$, we can determine the step widths for about 140 different rotation numbers.[5] Likewise we make use of the fact that the fractal dimension can be calculated from the number $N(r)$ of steps larger than a given scale r. In Ref. 5 we discussed the problems involved in using the original method where the sum of stability intervals $S(r)$ larger than a given scale r is measured. The main problem there is how to obtain the correct value of the total length of all the stability intervals in the considered region since the critical line bends. Besides, we would like to point out that only in the complete case will the two methods give the same result. If the step widths are measured too small (as would be the case if noise is present) the measured fractal dimension will approach 1 for the original method in contrast to the counting procedure where the measured fractal dimension will approach 0. The measurement has again been performed taking all steps between the 0/1 and 1/1 steps into account. The results are plotted in Fig. 8. The fractal dimension given by the slope is found to be $D=0.86\pm 0.02$. This is in agreement with our previous result on the sinusoidal $I(\phi)$ relation and the value obtained for the "sine" map[1,2] with a third-order nonlinearity

$$\phi_{n+1}=\phi_n+\Omega-\sin\phi_n\ . \tag{5}$$

For small values of r the effect of noise can clearly be observed as the points start bending over towards zero slope.

Two other universal numbers have been derived for the sine map. These are decay constants for the $1/Q$ step se-

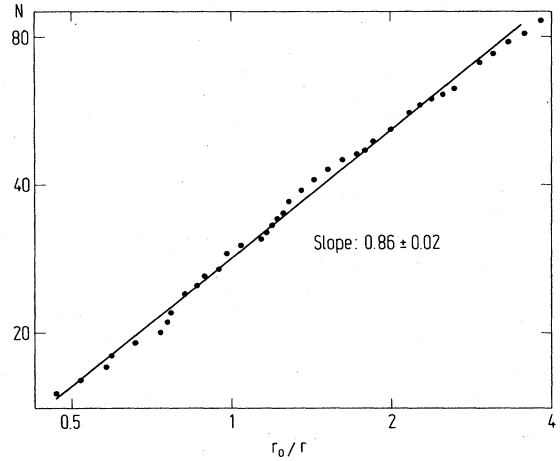

FIG. 8. The number $N(r)$ of steps larger than the scale r plotted versus r_0/r in a double-logarithmic plot, where $r_0=0.004$, for $I_B(\phi)=\sin(\phi+0.25\sin\phi)$.

quence[2] and for the Fibonacci sequence,[19] which latter sequence converges upon the golden mean. The numbers obtained are, respectively, $\delta=3$ and $y=2.164$. In this connection it is worth mentioning that while the fractal dimension D is expected only to depend on the order of the zero-slope inflection point in the return map, the decay exponent δ will depend on the behavior of the return map in the neighborhood of a point where the slope is one. In Fig. 9 the step sizes of the $1/Q$ substeps ($5 \leq Q \leq 16$) measured at the critical line is plotted as function of Q in a double-logarithmic plot. We find the decay constant to be $\delta=3.09\pm0.08$. For the Fibonacci sequence we find $y=2.3\pm0.2$. As in the case of the sinusoidal $I(\phi)$ relation we find quite good agreement.

So even though the critical line has moved a great deal and the substeps have become more prominent, along the critical line the scaling features have not changed. One might argue that even though $I(\phi)$ has become skewed, the nonlinearity is still of third order around the origin. But this would indicate that there is a way to connect the discrete return map to the properties of the nonlinearity. From the analysis of the data as displayed in Fig. 2, one can see that the inflection point is actually very close to $\phi_n=0$ (in Fig. 7 the zero has been arbitrarily shifted in order to better display the plateau around the inflection point of zero slope). One might therefore naively suspect that there is an intimate connection between the order of the nonlinearities at the inflection points for the map and for the $I(\phi)$ relation. As we shall show in the next section this notion is false.

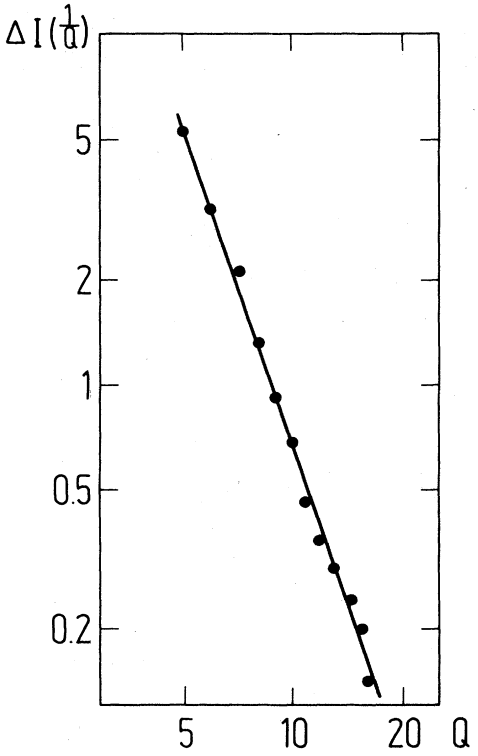

FIG. 9. The size of the $1/Q$ substeps along the critical line as function of Q plotted in a double-logarithmic plot for $I_B(\phi)=\sin(\phi+0.25\sin\phi)$. The slope is $\delta=3.09\pm0.08$. $A=1$ and $\omega=1.76$.

V. THE ORDER OF THE INFLECTION POINT

The fractal dimension related to a discrete circle map is known to depend on the order of the nonlinearity; e.g., $D=0.80\pm0.01$ for a fifth-order nonlinearity. $I(\phi)$ as given in Eq. (4) is of this type. We have therefore investigated the influence of this $I(\phi)$ relation. In the unperturbed case the I-V curve lies slightly below that for the sinusoidal $I(\phi)$ relation. This can be seen from the arguments in Sec. II. When the ac term is added the critical line is observed to fall below that for the sinusoidal $I(\phi)$ relation for high G values. For low G values the lines again run together.

We have again measured the fractal dimension by use of the counting method. The result is displayed in Fig. 10. The slope is here again found to be $D=0.87\pm0.02$. This value is distinctly different from 0.80 ± 0.01 which is found for a discrete circle map with a fifth-order nonlinearity[2] and in fact also from the values of D found for higher orders of the nonlinearity.[6] This dispels any doubts one might have harbored about the universality of the fractal dimension as relating to continuous dissipative physical systems. Truly there might locally be regions where a fifth-order inflection point accidentally comes into play, but a system has to be extremely weird for this to happen globally. In contradistinction to systems having a discrete dynamics, probably all dissipative systems with a continuous dynamics (i.e., a continuous time development), which exhibit chaos connected with mode locking, will have a fractal dimension of 0.87 along the critical line, whatever the shape of the periodic potential. This is very likely connected with symmetry breaking.

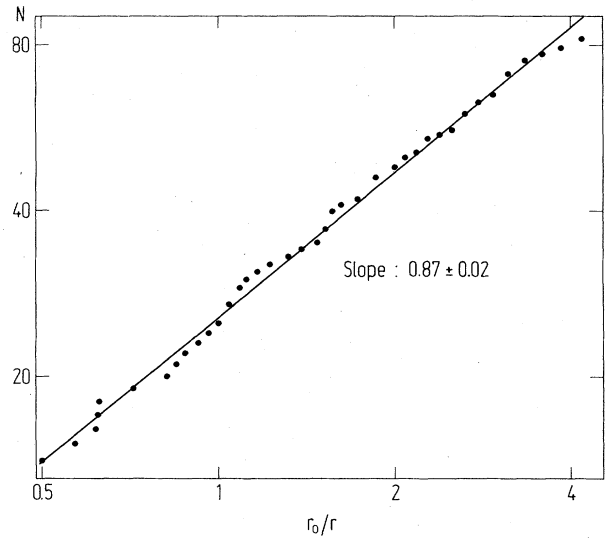

FIG. 10. The number $N(r)$ of steps larger than r plotted versus r_0/r in a double-logarithmic plot ($r_0=0.004$) for $I_5(\phi)=\frac{6}{7}(\sin\phi+\frac{1}{6}\sin^3\phi)$.

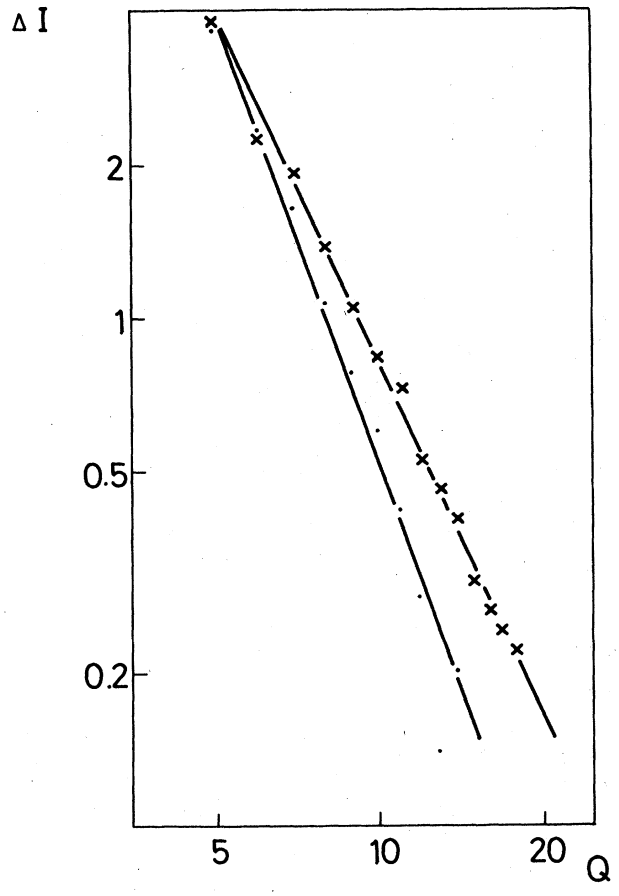

FIG. 11. The size of the $1/Q$ substeps (●) and the average over P of the P/Q substeps (×) along the critical line as function of Q plotted in a double-logarithmic plot for $I(\phi)=I_5(\phi)$. The slope is, respectively, $\delta=2.98\pm0.08$ and $\bar{\delta}=2.30\pm0.03$. $A=1$ and $\omega=1.76$.

In this case we have also investigated the decay exponents of the $1/Q$ sequence (Fig. 11) and the Fibonacci sequence. For these we find $\delta=2.98\pm0.08$ and $y=2.1\pm0.2$. These numbers are again very close to those predicted for the sine map.

VI. SELF-SIMILARITY

Although one might expect the devil's staircase locally to be self-similar at least in the regime of $G>1$, where the critical line runs nearly parallel to individual I-V characteristics, there is no reason to expect this to be true globally. From Fig. 6 it is seen that the dc current at the critical line first increases and then goes down again. Step widths are measured in units of the applied dc current. Since the rotation number W in the case of the discrete circle map is a monotonically increasing function of the "dc drive" Ω, there is no easy connection between the two parameters I and Ω. The scaling of Ω must change along the critical line, and it is therefore somewhat surprising that the fractal dimension when measured globally comes out right. However, if the change in scaling is smooth it is reasonable to believe that the fractal dimension is unchanged, but that the self-similarity only will exist locally.

There is another universal decay exponent $\bar{\delta}$ connected to a fractal dimension $\bar{D}$ ($\bar{D}=2/\bar{\delta}$) defined in a way different from the definition of D. This seems to be more intimately connected with the degree of global self-similarity. This decay exponent is found by taking the average with respect to P of the step widths $\Delta I(P/Q)$. These values are then considered as function of Q and shown in Fig. 11. If the P/Q step widths only depend on Q as is the case for the one-dimensional Ising model with long-range antiferromagnetic interaction, it is easy to verify that $\bar{D}=D$.[20] But in the cases considered here the P/Q steps depend on both P and Q. There is therefore no *a priori* reason why $\bar{D}$ should be equal to D even for the sine map, where indeed the fractal dimensions are found to be identical.[2] One would, however, expect $\bar{D}$ to be more likely to suffer from a scaling of Ω. From Fig. 10 we find $\bar{\delta}=2.30\pm0.03$, which is very close to the value of 2.29 found for the sine map. From $\bar{D}=2/\bar{\delta}$ we derive $\bar{D}=0.868\pm0.010=D$ within the experimental uncertainty. Table I shows a summary of our data for the different constants. As seen, there is an overall close agreement with the corresponding universal numbers for the sine map.

The result for $\bar{D}$ led us to plot the step widths as function of the rotation number W, see Fig. 12(a). For a comparison we also show the plot obtained for the sine map, Fig. 12(b). When one considers the dramatic change in the dc current along the critical line, the near perfect symmetry observed around the 1/2 step is truly surprising. Similar plots for the other $I(\phi)$ relations considered show the same degree of symmetry. Thus the complete devil's staircase found along the critical line is truly self-similar for $0/1<W<1/1$.

This strongly contrasts with the result on the CDW in $NbSe_3$ by Brown *et al.*[12] Their result[21] is shown in Fig. 12(c). It is evident that the substep structure is not self-

TABLE I. Summary of our data for the different constants.

$I(\phi)$	D	δ	y	$\bar{\delta}$	$\bar{D}$
$\sin\phi$	0.87 ±0.02	2.95±0.08	2.0 ±0.2	2.27 ±0.03	0.882±0.010
$\sin(\phi+0.25\sin\phi)$	0.86 ±0.02	3.09±0.08	2.3 ±0.2	2.29 ±0.03	0.873±0.010
$\sin\phi+\frac{1}{6}\sin^3\phi$	0.87 ±0.02	2.98±0.08	2.1 ±0.2	2.30 ±0.03	0.868±0.010
Return map given by Eq. (5), Refs. 2,19	0.8700±0.000 37	3.0	2.164 43±0.000 02	2.292±0.0034	0.873±0.0021

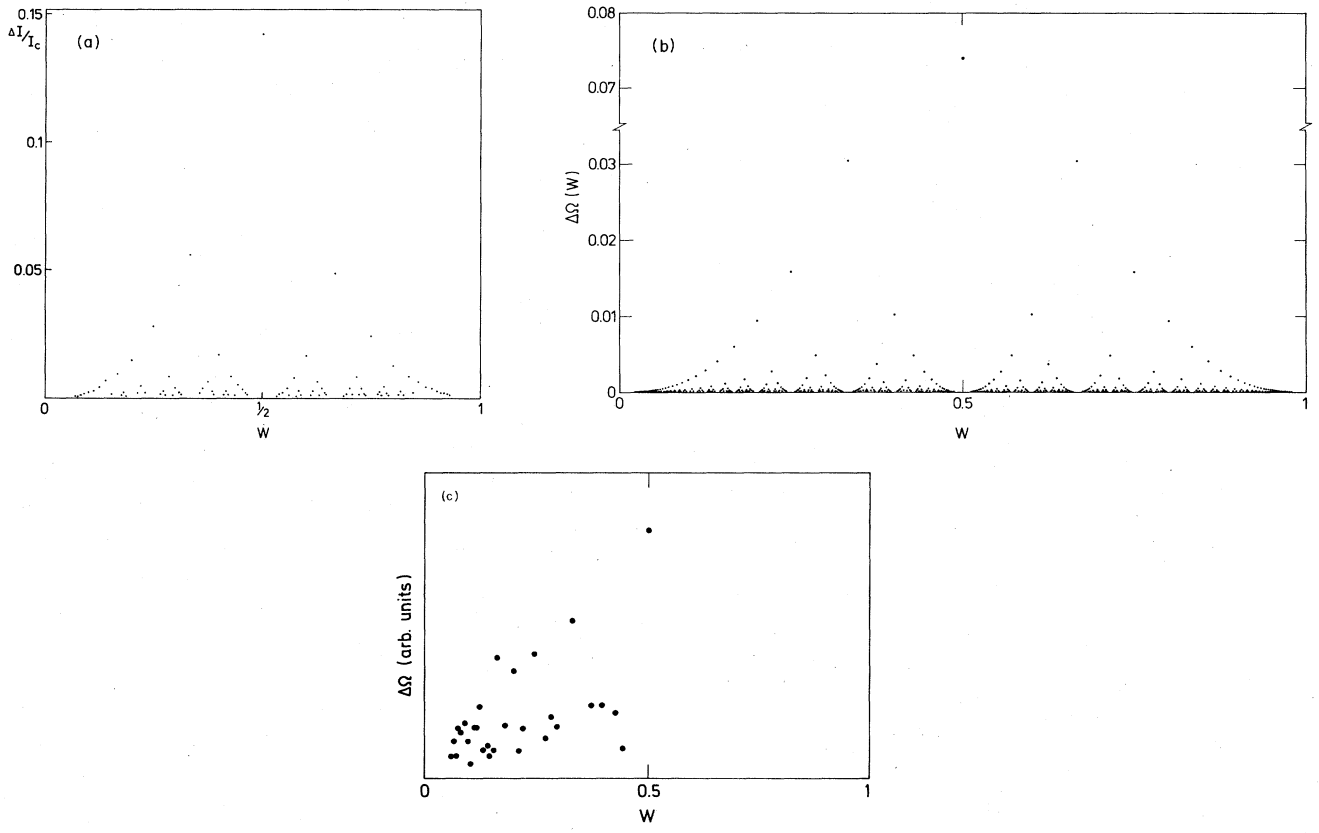

FIG. 12. The size of the substeps as function of the rotation number $W=P/Q$ between $0/1 < W < 1/1$ for (a) $I(\phi)=I_5(\phi)$. Note the remarkable symmetry and self-similarity. (b) For the sine map, Ref. 2. Note the break on the $\Delta\Omega$ axis. (c) For the CDW. Data from Ref. 21. Note the lack of self-similarity.

similar. No substeps are shown in the regime above the 1/2 step. From Fig. 2 in Ref. 12 it is clear that substeps exist also in this regime but are much less prominent than below the 1/2 step. This observation indicates that the fractal dimension is not measured along the critical line.

VII. CONCLUSIONS

In this work we have investigated the possibility of obtaining experimental proof for the universality of the fractal dimension of the complete devil's staircase and the related decay constants found for the driven damped-pendulum equation. With this in view we have discussed the effect of exchanging the sinusoidal potential with a periodic but nonsinusoidal. Our conclusion is that as long as the potential is periodic and chaos exists for finite rotation numbers, then the fractal dimension is $D=0.87$. We have furthermore found that the fractal dimension $\overline{D}$ evaluated by first taking the average with respect to P of the step widths $\Delta I(P/Q)$ is identical to D. The different decay constants are in all cases within experimental error found to be identical to those of the sine map.

A truly surprising result is the high degree of self-similarity found for the devil's staircase for all the different current-phase relations. Since the critical curve in (I,G) space bends back on itself, this was definitely not to be expected.

The conclusions mean that any dynamical system that shows chaos of this type can be used to actually measure the universal numbers. Josephson junctions have been regarded as providing an excellent opportunity. However, it is rather difficult to bring the parameters into the right regime without using external shunts that automatically change the differential equation into a more complicated form than the simple pendulum equation. However, one might now use tunnel junctions with external resistive shunts, microbridges, or *SNS* junctions with external capacitive shunts or point contacts with equal confidence. Also sliding charge-density-wave systems, where the dynamics are still unclear, can now with confidence be used to check the universality.

ACKNOWLEDGMENTS

We want to thank P. V. Christiansen and M. H. Jensen for valuable discussions. This work has been supported by the Danish Natural Science Research Council.

[1]P. Bak, T. Bohr, M. H. Jensen, and P. V. Christiansen, Solid State Commun. **51**, 231 (1984).
[2]T. Bohr, P. Bak, and M. H. Jensen, Phys. Rev. A **30**, 1970 (1984).
[3]W. J. Yeh, Da-Ren He, and Y. H. Kao, Phys. Rev. Lett. **52**, 480 (1984).
[4]P. Alstrøm, M. H. Jensen, and M. T. Levinsen, Phys. Lett. **103A**, 171 (1984).
[5]P. Alstrøm and M. T. Levinsen, Phys. Rev. B **31**, 2753 (1985).
[6]P. Alstrøm, Commun. Math. Phys. (to be published).
[7]P. E. Gregers-Hansen, E. Hendricks, M. T. Levinsen, and G. Fog Pedersen, *Proceedings of the Applied Superconductivity Conference, Annapolis, 1972* (IEEE, New York, 1972), p. 597.
[8]C. A. Hamilton and E. G. Johnson, Phys. Lett. **41A**, 393 (1972).
[9]V. N. Belykh, N. F. Pedersen, and O. H. Sørensen, Phys. Rev. B **16**, 4860 (1977).
[10]A. Zettl, C. M. Jackson, and G. Grüner, Phys. Rev. B **26**, 5773 (1982).
[11]R. P. Hall, M. Sherwin, and A. Zettl, Phys. Rev. B **29**, 7076 (1984).
[12]S. E. Brown, G. Mozurkewich, and G. Grüner, Phys. Rev. Lett. **52**, 2277 (1984).
[13]M. T. Levinsen, Rev. Phys. Appl. **9**, 135 (1974).
[14]L.-E. Hasselberg, M. T. Levinsen, and M. R. Samuelsen, Phys. Rev. B **9**, 3757 (1974); J. Low Temp. Phys. **21**, 567 (1975).
[15]P. Mukhopadhyay, Phys. Rev. B **17**, 402 (1978).
[16]P. E. Gregers-Hansen, M. T. Levinsen, and G. Fog Pedersen, J. Low Temp. Phys. **7**, 99 (1972).
[17]A. H. Dayem and J. J. Wiegand, Phys. Rev. **155**, 419 (1967).
[18]D. S. Fisher, Phys. Rev. Lett. **50**, 1486 (1983); R. A. Klemm and J. R. Schieffer, *ibid.* **51**, 47 (1983).
[19]S. J. Shenker, Physica **5D**, 405 (1982).
[20]P. Bak and R. Bruinsma, Phys. Rev. Lett. **49**, 249 (1982); R. Bruinsma and P. Bak, Phys. Rev. B **27**, 5824 (1982).
[21]S. E. Brown, G. Mozurkewich, and G. Grüner (unpublished).